Bioinspired strategy for coordinating multiple unmanned aerial vehicles for surveillance tasks

1st Sara Satake
College of Information Sciences
University of Tsukuba
Tsukuba, Japan
sarasaori19@gmail.com

2nd Guilherme Nakahata
College of Information Sciences
University of Tsukuba
Tsukuba, Japan
guilhermenakahata@gmail.com

3rd Rodrigo Calvo
College of Information Sciences
University of Maringa
Maringá, Brazil
rcalvo@uem.br

***Abstract*—Among unmanned autonomous systems, unmanned aerial vehicles (UAVs) stand out due to their wide range of applications, including surveillance, agriculture, and traffic monitoring. Bioinspired algorithms play an important role in the development of navigation strategies, particularly Ant Colony Optimization (ACO) and its variants for multi-robot coordination, such as the Inverse Ant System-Based Surveillance System (IAS-SS). While IAS-SS has shown promising results for unmanned ground vehicles (UGVs), its application to UAVs remains limited. This work proposes an autonomous navigation strategy for multi-UAV surveillance tasks based on IAS-SS. Experiments are conducted in two scenarios: a basic setting with variations in agent flight altitudes, and an adaptive setting involving the addition and removal of agents during simulation. All experiments are performed in virtual environments and evaluated using statistical performance metrics. Results indicate that the repulsive pheromone mechanism enables effective agent readaptation, particularly in dynamic scenarios with changes in the number of agents.**

***Index Terms*—multiple UAV system, surveillance task, unmanned aerial vehicles, ant colony optimization, swarm systems**

I. Introduction

Although most of the applications involving UAVs are aimed at the military environment, such as reconnaissance and attack operations [1], in recent years, research involving their use in everyday situations has been growing and gaining popularity in various purposes such as surveillance, agriculture, traffic, among others [2].

Regarding surveillance, it can be said that this activity involves monitoring individuals, buildings or behaviors to collect, manage and even guide [3] information. Such an operation has become a much explored topic in the context of UAVs, and faces challenges, e.g., division of surveillance tasks, optimization of energy consumption and adjustments of standby plans [4]. Furthermore, these agents have other characteristics compared to other robots, such as the feasibility of adapting to changes in terrain and ground conditions, as is the case of UGVs [5].

The use of bioinspired strategies has great influence on the development of the work, in particular the ant colony optimization algorithm (ACO), which serves as the basis for other strategies, such as the Inverse Ant System-Based Surveillance System (IAS-SS), until then, applied only in UGVs, yet, presents satisfactory results in the context of coordinating multiple robots for surveillance of a location, in particular due to its ability to adapt to the behavior of agents in the environment in which are involved.

The general objective of this work is to develop an autonomous navigation strategy for multiple UAVs capable of performing surveillance tasks in a given environment. For this, we defined some specific objectives: to investigate the IAS-SS strategy, which presented satisfactory results during works involving UGVs, to define the virtual environment for simulations, to demonstrate the performance of the algorithm in experiments with different characteristics, to discuss and analyze the results through of statistical metrics and comparisons with other approaches.

This paper is organized as follows: In Section II, we present related works related to multi-agent systems. The IAS-SS strategy is focused in Section III. The proposed method is defined in Section IV. The coordination of multiple UAVs is presented in Section V. Experimental results are listed during Section VI. We discussed the main results in Section VII. Lastly, the final considerations and future works are highlighted in Section VIII.

II. Related Works

Multi-robot cooperative systems are widely applied in autonomous navigation, particularly in scenarios involving multiple UGVs. A common coordination strategy is formation control, in which agents interact to maintain a predefined structure [6]. Such cooperation is often inspired by biological systems, whose collective behaviors motivate the development of artificial societies with organized and intelligent behavior [7].

Several studies employ the Ant Colony Optimization (ACO) algorithm for multi-robot navigation. Cong and Ponnambalam [8] proposed a path-planning approach that outperformed a genetic algorithm variant in most tested maps. Rashid et al. [9] evaluated ACO in environments with varying obstacle densities, achieving shorter simulation times in more complex scenarios. Liu et al. [10] combined ACO with geometric optimization, reducing the risk of convergence to local optima.

In surveillance and environmental monitoring tasks, biologically inspired approaches are also prominent. Fute et al.

[11] investigated ACO-based patrolling strategies considering different agent initial distributions and evaluating metrics such as idle time, energy consumption, and communication.

Calvo [12] proposed the use of the IAS-SS algorithm in UGVs, achieving effective surveillance through pheromone repulsion and local mapping. Oliveira et al. [13] extended this approach by modifying the sensor and communication model, enabling information exchange among robots and improving mapping performance.

III. IAS-SS Algorithm

The strategy proposed by Calvo [12] is called Inverse Ant System-Based Surveillance System (IAS-SS), and uses the main concepts of an artificial system based in ant colonies [14]. One of the notable modifications that differs the algorithm from the original is the action of repulsion of the agent to the deposited pheromone while they are moving, contrary to the behavior performed in the ACO.

According to the pheromone deposited in the environment, the sensors detect such information, and the navigation controller performs the agents' repulsion behavior. Thus, this component provides the agent with the direction where the pheromone concentration is low. Once these actions are performed, the pheromone dispersion component is activated, causing the agent to deposit pheromone in the area of its current instant. It is important to point out that, for this approach, the pheromone is dispersed to a region covered by sensors attached to the agent, and not just in its current position, minimizing the possibility that it travels through unnecessary regions of the environment. The pheromone evaporation has no direct relationship with the agent, since this event happens naturally.

Initially, the agent receives pheromone and obstacle proximity information, which are used by the navigation controller and obstacle avoidance module. It is possible that the navigation controller does not provide an obstacle-free path in some cases. Therefore, it is important that the obstacle avoidance module redirects a new route only if the sensor detects an obstacle in a short distance.

The direction adjustment based on the pheromone present in the IAS-SS approach is defined by two mechanisms: Stochastic Sampling (SS) and Best Ranked Stochastic Sampling (BRSS). Both consider the amount of substance detected at the edges of the sensor present in the agent, however, with different weighting strategies for the received stimuli, which are defined below.

- Stochastic Sampling (SS)

Given an area covered by the sensors reach, a probability value is stipulated for each sensor, through the discrete angle A_r defined for its positioning in relation to the robot. The probability received by the angle A_r is inversely proportional to the presence of pheromone on its edge of the corresponding sensor, because, due to the characteristic of the IAS-SS approach, the lower amount of pheromone, the greater the interest in that region. Thus, the probability $P(r)$ for an angle A_r is calculated through Eq. 1.

$$P(r) = \frac{1-\tau_r}{\sum_{i=-R}^{R}(1-\tau_i)} \quad (1)$$

where τ_r corresponds to the amount of pheromone on the edge of the discrete angle A_s of a given sensor.

For the adjustment of direction, a discrete random variable φ obtained through the probability $P(r)$, subject to values contained in the set

$$\{A_r | r = -R, ..., -1, 0, 1, ..., R\}$$

The direction adjustment is calculated by the Eq. 2 at every instant t.

$$\Omega_k(t) = \Omega_k(t-1) + \phi A_r^* \quad (2)$$

where $\Omega_k(t)$ is the movement direction of a robot k at instant t; $\phi \in$ [0,1] corresponds to the smoothing constant for adjusting the angle to the new direction and $A{*}_r$ is the value of a random variable φ at instant t for some $r = r*$, that is, the defined direction given probability calculated in Eq. 1.

- Best Ranked Stochastic Sampling (BRSS)

In this method, there is no consideration of all angular ranges of the sensors, as in the case of Stochastic Sampling. In order to improve decision-making to define the new direction, smaller sets of possibilities are designated. Two subsets U and V of the A_r sector are defined, with U containing elements from the circular sector A_r associated with the smallest amounts of the substance perceived by the sensor, and V containing randomly chosen elements from the circular sector and that are not present in U. Subsets are given specifications for their compositions:

label=$*$

- Subset U: if $A_r \in U$ and $A_z \notin U$, then $\tau_r \leq \tau_z$.
- Subset V: if $A_r \in V$, then $A_r \notin U$, and A_r is chosen randomly.

where τ_r is the pheromone rate in the angular range of A_r and r, where $z \in -R$,...,-1,0,1,...S .

A probability value is defined for each circular sector in both subsets U and V, which can be defined by Eq. 3.

$$Environment\overline{P(r)} = \frac{1-\tau_r}{\sum_{i \in r | A_r \in (U \cup V)}(1-\tau_i)} \quad (3)$$

where τ_r is the amount of pheromone corresponding to the sector A_r.

IV. Proposed method

In this Section, we present the proposed method, including the virtual environment, settings regarding the UAVs, and their main modules.

Fig. 1. Distance sensor representation

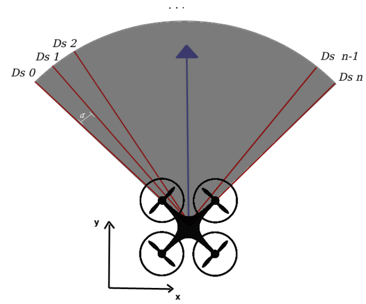

A. Virtual Environment

We use a virtual environment created in *Webots* [1](R2022b version) to support the presence of robots, as well as obstacles placed to perform tasks of surveillance, enabling the agents' movement mechanisms to occur in a way that meets the needs of a given function. The robot used for the development of the work is the drone DJI *MAVIC 2 Pro*.

For the elaboration of the surveillance system, we need to manipulate distance sensors to recognize obstacles and their possible deviation according to values obtained by reading the *lasers*, also defined for the set to be coupled to the UAV .

The distance sensors (Ds) perform the exploratory function, in parallel to the dispersion of the pheromone. The positioning of the sensors in relation to the UAV was strategically designed to cover its frontal area, since, due to the propellers playing a key role in the UAV locomotion mechanics, it is important that they are not subject to collisions with possible obstacles; otherwise, agent movement may be compromised. In this way, the sensors were connected from the point of origin of the drone. The distribution of the *lasers* is given in order to understand the sector corresponding to the left and right front propellers, according to a radius R, starting from the first sensor (Ds_0) to the last one (Ds_n) with angles of 0.69812*rad* and 5.41043*rad*, respectively, in relation to the UAV. The n sensors are placed at an identical distance of αrad, grouped in a set L in that interval. Figure 1 shows the distribution of sensors.

B. Navigation and exploration module

Bresenham's algorithm [15] allows lines to be drawn, in a matrix context, and determines which coordinates should be highlighted according to a certain degree of inclination of an angle in relation to the Cartesian plane. In this context, it is necessary to define the initial coordinates (X_0, Y_0) and final coordinates (X,Y), which, for the present work, are represented as the current position of the drone and coordinates relevant to the range of the sensor, in that order. Eq. 4 and 5 present the calculation for obtaining the abscissa and ordinate values of the extreme range points of a sensor $Ds \in L$, respectively.

[1]https://cyberbotics.com/

$$X = \cos(\beta) * d + X_0 \tag{4}$$

$$Y = \sin(\beta) * d + Y_0 \tag{5}$$

where β corresponds to the angle of a sensor in relation to the UAV, and d to the distance from the beginning of the sensor beam to its end. By obtaining the values (X, Y) of each sensor, the algorithm can be applied to carry out the mapping.

C. Obstacle avoidance module

As mentioned, the UAVs' propellers directly compromise the functioning of their agents for their handling tasks. Thus, they must have the ability to avoid any obstacles detected at a minimum distance by one of their lasers.

In situations where one or more lasers indicate the presence of a very close obstacle, the UAV stops its movement, performs a smooth retreat, performs a clockwise rotation on its own axis, and does not receive stimuli from the environment until for this module to be completed.

D. Pheromone release module

Pheromone release occurs according to distance sensors. Similar to the navigation and exploration module, given a set of L sensors, these carry out the task of pheromone allocation according to the range of their rays, through the coordinates highlighted by the Bresenham algorithm. The amount of pheromone is high near the beginning of the sensors, and decreases as the beam distance increases. Eq. 6 and 7 present the procedure for calculating deposited pheromone.

Let S_t be the sensor coverage area in the iteration t, Q be the complete surface of the environment, such that $S(t) \subset Q \subset R^2$, the amount of pheromone $\Delta_q^k(t)$ deposited by the kth drone in iteration t and position $q \in Q$ is given by:

$$\Delta_q^k(t) = (\tau_{max} - \tau_q(t-1))\Gamma_q^k(t), \text{ and} \tag{6}$$

$$\Gamma_q^k(t) = \begin{cases} \delta e^{\frac{-(q-q_k)^2}{\lambda^2}}, \text{ if } q \in S_t^k \\ 0, \text{ otherwise} \end{cases} \tag{7}$$

E. Pheromone evaporation

Since it is a volatile substance, like the biological, the virtual pheromone must be subject to the evaporation process. At each new iteration of the agents, the total amount of pheromone present in the environment is evaporated through the Eq. 8, with the evaporation rate being a variable value between 0 and 1.

$$\omega_q(t) = \mu \tau_q(t) \tag{8}$$

where $\omega_q(t)$ is the amount of pheromone to be evaporated at position q at instant t; μ, such that $0 \leq \mu \leq 1$ is the evaporation rate; and τ_q corresponds to the total pheromone in a position q, at time t.

Fig. 2. Behavioral flowchart of the proposed UAV navigation model

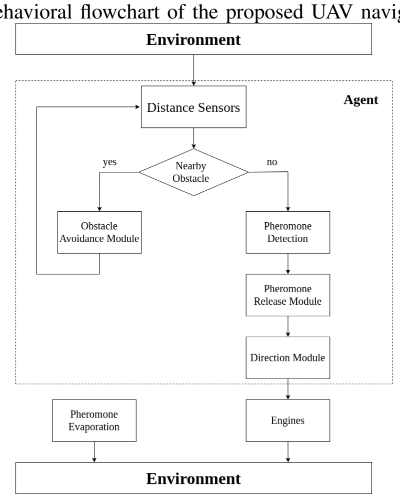

F. Direction module

Decision making regarding the UAV's direction depends on two factors: the presence of nearby obstacles and pheromone perception. When no obstacle is detected, direction is adjusted according to the pheromone level sensed, with lower values being more attractive. Otherwise, the obstacle avoidance module is activated. Figure 2 illustrates the behavioral flow of the proposed model.

V. COORDINATION OF MULTIPLE UAVS

A key factor in relation to the adaptations of ground vehicles to air vehicles concerns the consideration of the variable referring to the vertical displacement of agents while carrying out their navigation tasks, and, consequently, other functions such as surveillance in environments with different characteristics, which can be subject to changes involving different levels of heights to be considered.

The present work aims to use the particularity of the independence of locomotion by ground offered by UAVs, including diversification of altitudes over the area to be explored. Considering the IAS-SS strategy, which employs the pheromone allocation in a position q at an instant t for a plane $M(x, y)$, and this plane also receives the positioning of the agents that traverse it so two-dimensional, at a height h in relation to the surface, the proposed model considers this same plane as a global perspective, and that each agent operating at a different height is contained in a new independent plane $H(x, y)$, however, with stimuli received by the global plane and in which it is contained.

VI. COMPUTATIONAL EXPERIMENTS

The experiments were run on three workstations with the same requirements. The operating system was Ubuntu 20.04.4, 32GB of RAM, Intel(R) Xeon(R) processors, CPU E5-1650 v3 @ 3.50GHz, 12 CPUs and Webots version R2022b.

Surveillance of an environment is considered complete when it has all of its areas visited. At that moment, it is understood that a surveillance **cycle** has been completed, and then a new cycle begins.

All experiments were performed in two virtual environment layouts, with different compositions. The total area available for the robots in both environments is 20×20 meters and consists of **rooms** that partition the environment through walls with a height of 6 meters.

Each room is divided into small grid areas called **cells**, which correspond to a set of coordinates grouped to a parameterizable value. When all cells are visited at least once, a surveillance cycle is complete. Fig. 3 shows the divisions of the rooms listed, and their breakdown into cells for Environment 1 (Fig. 4(a)) and Environment 2 (Fig. 4(b)).

Fig. 3. Cell matrix representation for Environments 1 and 2

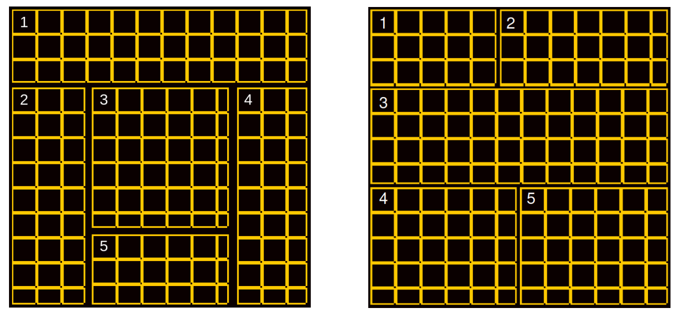

(a) Environment 1

(b) Environment 2

A. Settings

For the analysis of the behavior of the UAVs according to the IAS-SS strategy, we carried out some initial experiments in order to present different virtual environments, as well as the disposition and number of active agents.

During these experiments, 6 drones positioned in the initial rooms (room 1 for Environment 1, and room 3 for Environment 2) are set up, which move at a maximum speed of $0.1m/s$, with a decrease and stoppage of displacement when the obstacle avoidance module is activated. The number of distance sensor lasers is 31, allocated every $\alpha = 0.04654rad$, with a 4 meter range. If a sensor indicates a distance $DistMinimum < 1.5$, the obstacle avoidance is performed.

The amount of cells generated for Environment 1 at the instant $t(0) = 0$ is equal to 26, and 34 for Environment 2. A cell is a set of 30×30 coordinates (totaling 900 coordinates), which here we will call as full cell. A cell, when generated, must contain at least 50% of a complete cell to be considered able to be in the environment, since very small cells can compromise the dynamics of the robots, which, due to obstacle avoidance, may not visit that small region.

One experiment corresponds to a run of 6000 iterations. Thus, 10 experiments were generated for each addressed direction adjustment mechanism (SS and BRSS).

B. Experiments with uniform height

In these experiments, all UAVs operate at a height of 1 meter in relation to the ground, starting with the activation of the motors and their vertical stabilization; pheromone evaporation rate is 10% every 3 iterations. The experiments were carried out so that we analyzed when the UAVs were in the same perspective plane.

C. Experiments with pair heights

For experiments with pair heights, 3 different heights are used every 2 UAVs, they are: 0.5, 1.5 and 2.0 meters, with a pheromone evaporation rate of 10% every 3 iterations. In this scenario, we evaluated the sharing of two agents by height, considering their behavior in relation to the common plane, and towards others that are at different heights.

D. Experiments with distributed heights

In these experiments, each UAV operates at a different height, totaling 6 heights: 0.5, 1.0, 1.5, 2.0, 2.5 and 3.0 meters. In this way, each agent is responsible for a plan, and the behavior of the pheromones is analyzed as a global context, that is, all heights receive stimuli in relation to the release, perception and evaporation of pheromone together. An important differential in relation to previous experiments is that a robot does not intervene as an obstacle for another robot in their trajectories.

Table I shows the means and standard deviations (σ) for each experiments, with the SS and BRSS mechanisms for both environments.

TABLE I
MEAN AND STANDARD DEVIATION OF CYCLES PER EXPERIMENT

Experiment	Env.	Mech.	Mean	σ
Uniform Heights	1	BRSS	13.0	2.60
	1	SS	11.4	1.35
	2	BRSS	12.0	2.28
	2	SS	11.1	2.25
Pair Heights	1	BRSS	8.0	1.18
	1	SS	4.8	1.32
	2	BRSS	10.5	1.11
	2	SS	8.4	2.49
Distributed Heights	1	BRSS	10.1	1.13
	1	SS	5.3	1.90
	2	BRSS	9.3	3.57
	2	SS	7.7	2.00

E. Adaptive Experiments

In these experiments, we considered limitations present in unmanned vehicles, such as the useful life of a UAV to complete the tasks to which it was assigned. Therefore, two experiments are carried out: the first is related to the activation and, consequently, operation of the UAV after a certain period of time; and the second, simulates the shutdown of a UAV after a period of time in which it has been operating normally like the other agents, and thus remains inactive until the end of the execution. As observed during previous experiments, the BRSS decision-making method proved to be the strategy with the best number of cycles performed, requiring fewer iterations to carry them out. In this way, the BRSS method is defined for the subsequent experiments. The arrangement of agents follows the pattern established in experiments with distributed heights, emphasizing the characteristic of agents acting in different planes.

1) Addition of an agent: Given a set of 6 UAVs, 5 start the engines and take off to start the surveillance task at instant $t(0) = 0$ in the initial rooms, at position $p_0 \in Q$. The sixth UAV is activated after a certain period of time, in this case, after the instant $t = 3000$ interactions, out of a total of $t = 6000$ iterations.

Fig. 4. Heat maps for BRSS samples in Environments 1 and 2

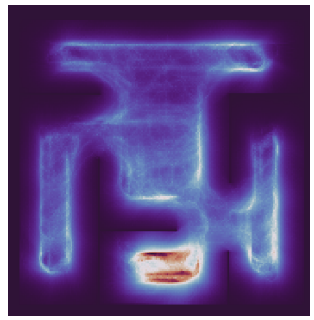

(a) Environment 1

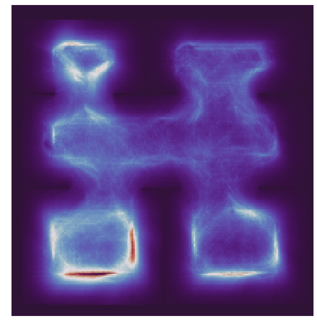

(b) Environment 2

TABLE II
MEAN AND STANDARD DEVIATION OF CYCLE COUNT

Experiment	Env.	Mean	σ
Addition of agent	1	12.1	1.57
	2	9.4	2.53
Removal of agent	1	8.2	1.53
	2	7.3	2.23

2) Removal of an agent: Similar to the previous experiment, the UAVs' behaviors are evaluated after a period of joint cooperation with initial training with a predefined number of agents, which is a set of 6 UAVs. In these experiments, however, all robots start their tasks at instant $t(0) = 0$, at position $p_0 \in Q$, remaining there for a certain period of time. From the instant $t = 3000$, an UAV is turned off, returning to the ground according to the last position $p_n \in Q$, and ends its contribution in the multi-agent system, until the execution is completed at the instant $t = 6000$.

Fig. 4 shows the map with the average pheromone concentration for the addition of an agent experiment for environments 1 and 2, where the concentrations over the rooms are similar to the other experiments.

Table II shows the means and standard deviations for each adaptive experiments.

VII. DISCUSSION

Through the results obtained with the different experiments, we pointed out the following particularities:

- The BRSS approach was the decision-making mechanism that most performed cycles, for all experiments, since it seeks to improve the SS approach, as it restricts the amount of possibilities of the steering module.

- Considering the basic experiments (uniform, pairs and distributed heights), the BRSS carried out surveillance cycles with a reduction of 29.06% in the number of iterations when compared to the SS.
- The experiment with uniform height was the one that presented the highest number of cycles, and as observed in the previous item, all UAVs are in the same plane, with no overlaps.
- It was noticed that, when the UAVs pass through the same place, they tend to keep a concentrated pheromone trail, this is due to the dispersion characteristic being a Gaussian function, in this way, the greater amount of the pheromone is also observed in nearby areas to the walls of the rooms.
- Adaptive experiments showed that the IAS-SS algorithm was able to adapt to the proposed scenarios, with the exploration of rooms performed satisfactorily. The adaptation of the agents in being able to carry out the surveillance task in these experiments was possible due to the characteristic of the pheromone used, thus being able to make agents use the pheromone already present even before starting their operation.
- When analyzing the experiments with the addition of an agent, quantities of cycles greater than the baseline experiments of pairs and distributed heights were obtained. One justification is again related to the pheromone, which is scattered throughout the map; and from the moment the sixth agent starts his surveillance tasks, there is a tendency to move to the area with less pheromone.

VIII. Conclusion and Future Works

The present work addressed a surveillance system for unmanned aerial vehicles (UAVs). We investigated the IAS-SS strategy, which consists of a variation of the ant colony algorithm (ACO). The main differential concerns the repulsive behavior of the agents towards the pheromone, contrary to the original algorithm. The IAS-SS proved to be an algorithm capable of acting in systems for surveillance tasks, presenting satisfactory results in studies that used it, these being exclusively with the use of unmanned ground vehicles (UGVs). Due to the results already obtained with this nature, it is proposed that the algorithm be adaptable for UAVs, considering the limitations and adaptations for this medium. The experiments are performed based on two strategies for decision making regarding the driving module: the SS and BRSS strategies.

We pointed out some characteristics for the experiments, such as the number of heights to be considered, as well as issues related to adaptive behavior. The UAVs showed good results when they are subject to uniform heights, since it is not possible for an agent to act in the same vertical plane as another agent, as is the case with different heights, which, as it is a probabilistic strategy, there is the possibility of one or more agents act on the same vertical axis. However, the experiments that used different heights showed results close to those obtained with the same heights, solidifying the repulsive property of the pheromone.

Furthermore, when considering situations such as the addition or removal of agents, the algorithm also proved to be effective in providing the adaptation of the agents to the environment through the stimuli received by the sensors, and eventual habituation of the pheromone indices present. When simulated cases with the removal of an agent, however, there was a higher incidence of agents operating in the same room.

For future work, we intend to: Implement the Gaussian function for pheromone dispersion, so that heights have greater interference according to other UAVs, for example, the pheromone released by an UAV acting at a height of 3.0m exerts a greater influence for an UAV at 2.0m than for an UAV at 0.5m from the ground; use UAVs with heterogeneous characteristics, with different sizes, speed and flight capacity; perform experiments with different initial positions of the agents at the beginning of simulations and consider the partitioned IAS-SS strategy.

References

[1] J. Zhang, Y. Wu, W. Liu, and X. Chen, "Novel approach to position and orientation estimation in vision-based uav navigation," *IEEE Transactions on Aerospace and Electronic Systems*, vol. 46, no. 2, pp. 687–700, 2010.

[2] W. N. Tun, M. Tyan, S. Kim, S.-H. Nah, and J.-W. Lee, "Marker tracking with ar drone for visual based navigation using surf and mser algorithms," in *KSAS 2017 Spring Conference*, 2017.

[3] X. Li and A. V. Savkin, "Networked unmanned aerial vehicles for surveillance and monitoring: A survey," *Future Internet*, vol. 13, no. 7, p. 174, 2021.

[4] C. Xu, K. Zhang, Y. Jiang, S. Niu, T. Yang, and H. Song, "Communication aware uav swarm surveillance based on hierarchical architecture," *Drones*, vol. 5, no. 2, p. 33, 2021.

[5] Y. Li, "Design and development of an interactive autonomous monitoring and surveillance drone," Ph.D. dissertation, 2020.

[6] A. Gautam and S. Mohan, "A review of research in multi-robot systems," in *2012 IEEE 7th International Conference on Industrial and Information Systems (ICIIS)*, 2012, pp. 1–5.

[7] M. Masar, "A biologically inspired swarm robot coordination algorithm for exploration and surveillance," in *2013 IEEE 17th International Conference on Intelligent Engineering Systems (INES)*. IEEE, 2013, pp. 271–275.

[8] Y. Z. Cong and S. Ponnambalam, "Mobile robot path planning using ant colony optimization," in *2009 IEEE/ASME International Conference on Advanced Intelligent Mechatronics*. IEEE, 2009, pp. 851–856.

[9] R. Rashid, N. Perumal, I. Elamvazuthi, M. K. Tageldeen, M. A. Khan, and S. Parasuraman, "Mobile robot path planning using ant colony optimization," in *2016 2nd IEEE International Symposium on Robotics and Manufacturing Automation (ROMA)*. IEEE, 2016, pp. 1–6.

[10] J. Liu, J. Yang, H. Liu, X. Tian, and M. Gao, "An improved ant colony algorithm for robot path planning," *Soft computing*, vol. 21, no. 19, pp. 5829–5839, 2017.

[11] E. T. Fute, E. Tonye, F. Lauri, and A. Koukam, "Multi-agent patrolling: Multi-objective approach of the event detection by a mobile wireless sensors network," *International Journal of Computer Applications*, vol. 88, no. 12, 2014.

[12] R. Calvo, "Sistemas bio-inspirados para coordenação de múltiplos robôs móveis," Ph.D. dissertation, Universidade de São Paulo, 2012.

[13] J. R. Oliveira, R. Calvo, and R. A. Romero, "Integration of virtual pheromones for mapping/exploration of environments by using multiple robots," in *5th IEEE RAS/EMBS International Conference on Biomedical Robotics and Biomechatronics*. IEEE, 2014, pp. 835–840.

[14] M. Dorigo, "Optimization, learning and natural algorithms," *Ph. D. Thesis, Politecnico di Milano*, 1992.

[15] J. E. Bresenham, "Algorithm for computer control of a digital plotter," *IBM Systems Journal*, vol. 4, no. 1, pp. 25–30, 1965.